Extending the kinetic solution of the classic Michaelis–Menten model of enzyme action

**Jose Ailton Conceicao Bispo · Carlos Francisco Sampaio Bonafe ·
Volnei Brito de Souza · João Batista de Almeida e Silva ·
Giovani Brandao Mafra de Carvalho**

Abstract The principal aim of studies of enzyme-mediated reactions has been
to provide comparative and quantitative information on enzyme-catalyzed reactions
under distinct conditions. The classic Michaelis–Menten model (Biochem Zeit 49:333,
1913) for enzyme kinetic has been widely used to determine important parameters
involved in enzyme catalysis, particularly the Michaelis–Menten constant (K_M) and
the maximum velocity of reaction (V_{max}). Subsequently, a detailed treatment of the
mechanisms of enzyme catalysis was undertaken by Briggs–Haldane (Biochem J
19:338, 1925). These authors proposed the steady-state treatment, since its applicabil-
ity was constrained to this condition. The present work describes an extending solution
of the Michaelis–Menten model without the need for such a steady-state restriction.
We provide the first analysis of all of the individual reaction constants calculated ana-
lytically. Using this approach, it is possible to accurately predict the results under new

J. A. C. Bispo (✉)
Departamento de Tecnologia (DTEC), Faculdade de Engenharia de Alimentos, Universidade Estadual
de Feira de Santana (UEFS), CP 252/294, Feira de Santana, BA, CEP 44036-900, Brazil
e-mail: jose.a.c.bispo@gmail.com

C. F. S. Bonafe
Departamento de Bioquímica, Instituto de Biologia, Laboratório de Termodinâmica de Proteínas,
Universidade Estadual de Campinas (UNICAMP), CP 6109, Campinas, SP, CEP 13083-970, Brazil

V. B. de Souza · G. B. M. de Carvalho
Departamento de Tecnologia (DTEC), Faculdade de Engenharia de Alimentos, Laboratórios de
Engenharia Bioquímica e Operações Unitárias III, Universidade Estadual de Feirade Santana (UEFS),
CP 252/294, Feira de Santana, BA, CEP 44036-900, Brazil

J. B. de Almeida e Silva
Departamento de Biotecnologia (DeBiq), Escola de Engenhariade Lorena (EEL), Universidade de São
Paulo (USP), CP 116, Lorena, SP, CEP 12600-970, Brazil

experimental conditions and to characterize and optimize industrial processes in the fields of chemical and food engineering, pharmaceuticals and biotechnology.

1 Introduction

The process in which a substrate S undergoes transformation to product P by enzyme activity E has been extensively studied during the last century. O'Sulivan and Thompson [1] provided one of the earliest formal studies on enzymology in which they demonstrated that the rate of reaction was proportional to the amount of enzyme [2]. Subsequent analysis by Brown [3] and Henri [4,5] focused on the formation of an *enzyme-substrate* complex. Their findings led Michaelis and Menten [6] to realize the need for additional experiments in order to solve the theoretical divergences between the Brown and Henri models. The work of Michaelis and Menten led these authors to propose a model of enzyme action in which S is transformed into P by the action of E with the formation of an enzyme-substrate (*ES*) complex. The model proposed by these authors was formally described by Briggs and Haldane in 1925 [7] by using a series of reaction parameters. This approach, known as the steady-state treatment, is still used by several research groups. Currently, the investigation of enzyme kinetics before the steady-state be reached, i.e., pre-steady-state kinetics, is important for characterization of the first enzyme-substrate contact [8]. The use of special techniques also allows the study of the enzymatic activity of multi-state molecules, thus providing details of intermediate reaction steps. Kinetic studies themselves cannot deduce the mechanism of catalysis, but can suggest possible alternatives that can serve as a basis for future experiments aiming process optimization.

Peroxidase (EC 1.11.1.7; donor: hydrogen-peroxide oxidoreductase: POD) catalyzes the oxidation of a variety of substrates using hydrogen peroxide (H_2O_2) [9]. POD is a monomeric, glycosylated protein containing heme as a prosthetic group [10–13]. PODs are among the main enzymes responsible for the enzymatic deterioration of fruit and vegetable products. These enzymes catalyze the oxidation of polyphenol substances naturally present in raw materials to yield products responsible for changes in color and sensory and nutritional characteristics [14] . Peroxidase is one of the most heat-stable enzymes in fruit and vegetables. The low specificity for hydrogen donor substrates means that PODs can oxidize a variety of aromatic amines, e.g., o-dianisidine, and phenols, e.g., guaiacol, as well as other organic compounds, at the expense of H_2O_2 [14]. Some novel applications suggested for POD include the development of biosensors, treatment of waste water containing phenolic compounds, synthesis of various aromatic chemicals and removal of peroxide from materials such as foodstuffs and industrial wastes [15].

In this work, we describe an extension of the kinetic solution of [7] and use POD to corroborate this model of enzyme action. The treatment described here provides several important parameters that contribute to our understanding of enzymatic catalysis and may be useful in the design, optimization and control of bioreactors.

2 Materials and methods

2.1 Collection of crude enzyme

Pineapple was used as the source of POD. Prior to use, the fruit was washed in tap water, peeled and chopped into small pieces. Fifty grams of fruit was homogenized in a blender with 50 mL of 0.1 mol/L phosphate-buffered saline (NaCl, 1.0 mol/L), pH 6.0. The mixture was then filtered and centrifuged at 4,000 rpm for 20 min at 4°C. The supernatant solution was stored in a freezer and used as a source of POD.

2.2 Determination of peroxidase activity

POD activity was assayed as described by [16]. The substrate solution was prepared daily by mixing 0.1 mL of guaiacol, 0.1 mL of H_2O_2 (30%), and 99.8 mL of potassium phosphate buffer (0.1 mol/L, pH 6.5), with different final concentrations of guaiacol, according to the experiment. The substrate was mixed well by shaking vigorously for a few minutes. The reaction mixture consisted of 0.2 mL of enzyme extract and 3.30 mL of substrate solution in a quartz cuvette followed by stirring with a capillary glass rod. Peroxidase activity was measured based on the increase in absorbance at 470 nm using a spectrophotometer (Varian Cary 50 Probe). The reaction was monitored for 10 min. All of the experiments were done four times for each experimental condition and the average values were used for analysis. Enzyme activity was calculated from the change in absorbance (ΔA) at 470 nm, using the equation: $Act(U/L) = \Delta A \, per \, min \times TV \times 10^3 / \varepsilon \times SV \times PL$, where ΔA per min is the change in absorbance at $470 \, nm \, min^{-1}$, TV is the total volume (3.50 mL), ε is the molar extinction of tetraguaiacol at 470 nm ($2.66 \times 10^4 \, L \, mol^{-1} cm^{-1}$), SV is the volume of enzyme solution (0.2 mL), PL is the light pathlength (1 cm), and 10^3 is the conversion factor (mL and L^{-1}). One unit of activity was defined as the amount of enzyme that produced 1 mmol of tetraguaiacol min^{-1} under the assay conditions described here.

2.3 Determination of tetraguaiacol concentration

POD is a classic example of a 'Michaelian' enzyme since it is a monomer with a substrate binding profile that resembles the classic non-cooperative protein myoglobin [17]. POD converts guaiacol into the reaction product tetraguaicol, with the color of the substrate solution changing from transparent to dark red. This color change results in a continuous increase in absorbance that can be monitored continuously, with no need to interrupt the reaction. The tetraguaiacol concentration was calculated by subtracting the absorbance observed at each time interval (A_{med}) from the minimum absorbance (A_{min}) and dividing by ε, the molar extinction of tetraguaiacol at 470 nm($2.66 \times 10^4 \, L \, mol^{-1} cm^{-1}$), as follows: $C_P(t) = \frac{A_{med} - A_{min}}{\varepsilon}$, resulting in the experimental data in Fig. 1.
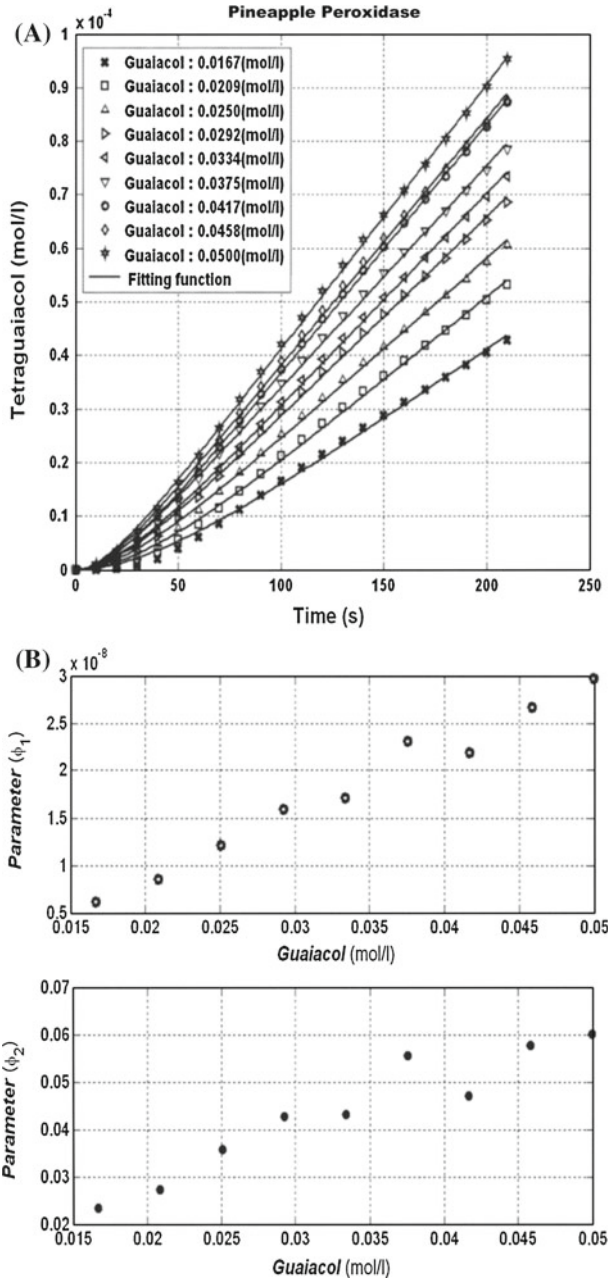
Fig. 1 a Initial adjustments of Eq. (45) to the experimental results of pineapple peroxidase for increasing substrate (guaiacol) concentration. **b** Values obtained for the parameters ϕ_1 and ϕ_2 at each substrate concentration

2.4 Determination of enzyme concentration

The POD concentration was determined spectrophotometrically (Varian Cary 50 Probe spectrophotometer) at 403 nm using an extinction coefficient ($\varepsilon^{1\%}$) of $1.02 \times 10^5 \, \text{cm}^{-1} \, \text{L} \, \text{mol}^{-1}$ [18]. The absorbance of the purified solution in the absence of substrate (guaiacol) was $\varepsilon^{1\%} = 0.025$ which yielded an enzyme concentration of 2.45×10^{-7} mol/L.

2.5 The steady-state treatment

According to the treatment proposed by Briggs and Haldane [7] for the Michaelis–Menten model of enzyme action (described below), the first constraint imposed on the model is that the initial substrate concentration is much higher than the initial enzyme concentration, i.e., $c_S \ggg c_E$:

$$S + E \underset{k_{-1}}{\overset{k_1}{\rightleftharpoons}} ES \overset{k_2}{\rightarrow} P + E \tag{1}$$

where S is the substrate, E the enzyme, P the product and ES the enzyme-substrate complex. The terms k_1, k_{-1} and k_2 are the respective reaction rate constants.

In addition to this constraint, there is the requirement for a steady-state in which the concentration of the ES complex does not change significantly with time. In this view, the concentration of any species in solution at any time is given by the extent of reaction (x_T) for the model in Eq. (1) as follows:

$$C_S(t) \approx c_S \tag{2}$$
$$C_E(t) = c_E - x_T(t) \tag{3}$$
$$C_{ES}(t) = x_T(t) \tag{4}$$

where C is the concentration of the species indicated by the subscript term at time t.

Since the substrate concentration is virtually constant, $C_S(t)$ is considered to be unchanged with respect to time. Since $\boldsymbol{x_T}$ represents the net number of moles of enzyme that in a specific time forms enzyme-substrate complex, the steady-state condition implies that:

$$v_T(t) = v_1(t) - v_{-1}(t) - v_2(t) = 0, \text{ so that}$$
$$v_1(t) = v_{-1}(t) + v_2(t) \Rightarrow k_1 c_S(c_E - x_T(t)) = k_{-1} x_T(t) + k_2 x_T(t) \tag{5}$$

where $v_T(t)$ is the total velocity of complex change at a given concentration, v_1 is the velocity of complex formation, v_{-1} is the velocity of complex dissociation and v_2 the velocity of product formation in accordance with Eq. (1).

Rearranging for x_T in Eq. (5) yields:

$$x_T(t) = \frac{k_1 c_E c_S}{k_{-1} + k_2 + k_1 c_S}$$

Since the velocity of product formation is given by:

$$v_2 = k_2 C_{ES}(t) = k_2 x_T(t)$$

we obtain the following relationship:

$$v_2 = \frac{k_1 k_2 c_E c_S}{k_{-1} + k_2 + k_1 c_S}$$

This relationship can be rewritten as the classic Michaelis–Menten equation if the following is assumed

$$v_2 = \frac{V_M c_S}{K_M + c_S} \tag{6}$$

where $K_M = \frac{k_{-1} + k_2}{k_1}$ is the Michaelis–Menten constant and $V_M = k_2 c_E$ is the maximum or limiting velocity.

Inspection of Eq. (6) shows that its integral form with respect to time and the initial conditions furnishes a straight line with the intercept at zero, as follows:

$$x_2 = \frac{V_M c_S}{K_M + c_S} t \tag{7}$$

Theoretically, this means that at $c_S \ggg c_E$ the product concentration (x_2) versus time is a straight line that intercepts the zero point of product and time. However, the intercept at the zero point is generally not observed in experimental conditions because of the assumed steady-state constraint. This in turn means that it is not possible to determine the kinetic behavior of the enzyme at early time intervals. Thus, despite numerous studies in this field, an analytical solution of this model without the steady-state constraint has so far not been reported. In what follows, we describe a general treatment reached by our group that allows characterization of the Michaelis–Menten model without the steady-state constraint. The solution described here makes it possible to assess many other important aspects of the behavior of the Michalis-Menten model and allows the optimization of industrial processes involving enzymes and microorganisms such as bacteria and yeast.

2.6 The proposed treatment

The Laplace transform is a tool that allows the conversion of differential equations systems into algebraic equations systems written in terms of the parameter 's'. Thus, after solving the algebraic equations, we used inverse Laplace transforms to find the differential solution. The solution proposed here also considers $c_S \ggg c_E$ but starts

as follows for the model in Eq. (1):

$$C_E(t) = c_E - x_1(t) + x_{-1}(t) + x_2(t) \tag{8}$$
$$C_{ES}(t) = x_1(t) - x_{-1}(t) - x_2(t) \tag{9}$$
$$C_P(t) = x_2(t) \tag{10}$$

where x represents the extent of reaction with the subscript indicating the orientation of the reaction. Therefore, if $x_L(t) = x_1(t) - x_{-1}(t)$, then it follows that

$$C_E(t) = c_E - x_L(t) + x_2(t) \tag{11}$$
$$C_{ES}(t) = x_L(t) - x_2(t) \tag{12}$$
$$C_P(t) = x_2(t) \tag{13}$$

For $x_T(t) = x_L(t) - x_2(t)$, Eqs. (11) and (12) reduce to Eqs. (3) and (4). Thus, without the steady-state restriction, we can solve this system by first considering the reaction velocities:

$$v_1(t) = \frac{dx_1(t)}{dt} = k_1 c_S (c_E - x_L + x_2(t)) \tag{14}$$

$$v_{-1}(t) = \frac{dx_{-1}(t)}{dt} = -k_{-1}(x_L(t) - x_2(t)) \tag{15}$$

$$v_2(t) = \frac{dx_2(t)}{dt} = k_2(x_L(t) - x_2(t)) \tag{16}$$

Subtracting Eq. (14) from (15) yields:

$$v_L(t) = \frac{dx_1(t)}{dt} - \frac{dx_{-1}(t)}{dt} = k_1 c_S c_E - (k_1 c_S - k_{-1})x_L(t) + (k_1 c_S - k_{-1})x_2(t) \tag{17}$$

Rearranging for $x_L(t)$ in Eq. (16) yields:

$$x_L(t) = \frac{1}{k_2}\frac{dx_2(t)}{dt} + x_2(t) \tag{18}$$

Differentiating Eq. (18) with respect to time yields:

$$v_L(t) = \frac{dx_L(t)}{dt} = \frac{1}{k_2}\frac{d^2 x_2(t)}{dt^2} + \frac{dx_2(t)}{dt} \tag{19}$$

Introducing Eqs. (18) and (19) into Eq. (17) yields

$$\frac{1}{k_2}\frac{d^2 x_2(t)}{dt^2} + \frac{dx_2(t)}{dt} = k_1 c_S c_E - (k_1 c_S - k_{-1})\left(\frac{1}{k_2}\frac{dx_2(t)}{dt} + x_2(t)\right)$$
$$+ (k_1 c_S - k_{-1})x_2(t)$$

and simplifying with respect to $x, \dot{x}, \ddot{x}$ in the previous equation results in:

$$\frac{d^2 x_2(t)}{dt^2} = k_1 k_2 c_E c_S - (k_1 c_S - k_{-1} + k_2) \frac{dx_2(t)}{dt} \tag{20}$$

Now, from the Laplace transforms and the initial conditions we obtain:

$$L\left(\frac{d^2 x_i(t)}{dt^2}\right) = s^2 X_i - s x_i(0) - \frac{dx_i}{dt}(0)_i \tag{21}$$

where $x_i(0) = \frac{dx_i}{dt}(0) = 0$. It follows that:

$$L\left(\frac{d^2 x_i(t)}{dt^2}\right) = s^2 X_i$$

$$L\left(\frac{dx_i(t)}{dt}\right) = s X_i - x_i(0) = s X_i \tag{22}$$

$$L\left(x_i(t)\right) = X_i \tag{23}$$

$$L\left(a\right) = \frac{a}{s} \tag{24}$$

where a is a constant

These equations can be applied to Eq. (20) to obtain the following relationship:

$$s^2 X_2 = \frac{k_2 k_1 c_S c_E}{s} - (k_1 c_S - k_{-1} + k_2) s X_2 \tag{25}$$

so X_2 corresponds to

$$X_2 = \frac{k_2 k_1 c_S c_E}{s^2(s + (k_1 c_S - k_{-1} + k_2))} \tag{26}$$

Since the term on the right of Eq. (26) does not appear in inverse Laplace transform tables it needs to be separated in terms of its partial fractions that are a function of the 's' terms, such that:

$$X_2 = \frac{k_2 k_1 c_S c_E}{s^2(s + (k_1 c_S - k_{-1} + k_2))} = \frac{A_1}{s} + \frac{A_2}{s^2} + \frac{B}{s + (k_1 c_S - k_{-1} + k_2)} \tag{27}$$

By calculating the parameters A_1, A_2 and B based on the selection of appropriate values for 's' to make both sides of Eq. (27) equal [19] we obtain:

$$A_1 = -\frac{k_1 k_2 c_E c_S}{(k_1 c_S - k_{-1} + k_2)^2}; \quad A_2 = \frac{k_1 k_2 c_E c_S}{(k_1 c_S - k_{-1} + k_2)};$$

$$B = \frac{k_1 k_2 c_E c_S}{(k_1 c_S - k_{-1} + k_2)^2} \tag{28}$$

Taking the inverse Laplace transform (L^{-1}) of Eq. (27) with the parameters in Eq. (28) yields:

$$L^{-1}\left(\frac{A_1}{s}\right) = A_1 \tag{29}$$

$$L^{-1}\left(\frac{A_2}{s^2}\right) = A_2.t \tag{30}$$

$$L^{-1}\left(\frac{B}{s+a}\right) = B\exp(-at) \tag{31}$$

where a is a constant, in this case equal to $(k_1 c_S - k_{-1} + k_2)$

Thus, the differential solution for the parameter $x_2(t)$ can be obtained by using the right term of Eq. (27) and appropriate tables of inverse Laplace transforms to give:

$$x_2(t) = \\ -\frac{k_1 k_2 c_E c_S}{(k_1 c_S - k_{-1} + k_2)^2} + \frac{k_1 k_2 c_E c_S}{(k_1 c_S - k_{-1} + k_2)}t + \frac{k_1 k_2 c_E c_S}{(k_1 c_S - k_{-1} + k_2)^2}e^{-(k_1 c_S - k_{-1} + k_2)t} \tag{32}$$

Differentiating Eq. (32) yields the velocity of product formation, $v_2(t)$:

$$v_2(t) = \frac{k_1 k_2 c_E c_S}{(k_1 c_S - k_{-1} + k_2)}\left(1 - e^{-(k_1 c_S - k_{-1} + k_2)t}\right) \tag{33}$$

By applying the definitions for V_M (Eq. 6) and K_G (Eqs. 32 and 33) we finally obtain:

$$v_2(t) = \frac{V_M c_S}{(K_G + c_S)}\left(1 - e^{-k_1(K_G + c_S)t}\right) \tag{34}$$

where

$$K_G = \frac{k_2 - k_{-1}}{k_1} \tag{35}$$

is the 'global' constant, so that

$$x_2(t) = -\frac{V_M c_S}{k_1(K_G + c_S)^2} + \frac{V_M c_S}{(K_G + c_S)}t + \frac{V_M c_S}{k_1(K_G + c_S)^2}e^{-k_1(K_G + c_S)t} \tag{36}$$

Inspection of Eq. (35) and comparison with Eq. (6) for K_M shows that these equations differ with respect to the sign of the rate constant k_{-1}. However, in this case, despite this difference in sign, the constant K_G is numerically equivalent to the K_M ($K_G \equiv K_M$) when $k_2 > k_{-1}$. The negative signal used here only indicates that the direction of the reaction is the opposite of that for the remaining reactions. Consequently, the global constant has the properties of a partition constant. Therefore, if K_G is negative, complex dissociation is greater than product formation. Similarly,

if $K_G = 0$, then complex dissociation and product formation have the same rate constants and, consequently, the same velocities and probability of occurrence. For $K_G > 0$, the rate of product formation is greater than that of complex dissociation. Consequently, since the literature values for K_M in many enzymatic processes are positive, we conclude that the rate of product formation in these cases will represent the slow stage of reaction when $v_L > v_2$ and $x_L > x_2$.

Inspection of Eq. (34) shows that its expression is more general than those obtained by Briggs and Haldane [7]. However, when the reaction time increases (t → ∞) and the steady-state is reached, this equation reduces to the Briggs and Haldane solution and to the Michaelis–Menten equation for enzyme kinetics. Eq. (34) also shows that in the steady-state that is reached when the third term on the right of Eq. (32) is zero or negligible, the straight line that fits the experimental conditions will only pass through the zero point of product and time if the intercept parameter is equal to zero. In this case, from Eq. (34) we have:

$$-\frac{V_M c_S}{k_1(K_G + c_S)^2} = 0$$

For cases where this intercept parameter is not zero, Eq. (36) becomes useful for calculating the other kinetic parameters that are not provided by the Briggs and Haldane treatment. The Monod equation for fermentation [20] also expresses this time dependency since the theoretical foundation of the Monod equation is the same as the Michaelis–Menten equation. This, in turn, makes it possible to access information that is not provided by the Michaelis–Menten and Briggs–Haldane treatments.

Since we have now characterized the model, we can now introduce Eqs. (36) and (34) into Eq. (18). The resulting equation allows us to obtain $x_L(t)$ and, after differentiation, to calculate $v_L(t)$, as follows:

$$x_L(t) = \frac{c_E c_S(k_1 c_S + k_{-1})}{k_1(K_G + c_S)^2} + \frac{V_M c_S}{(K_G + c_S)}t - \frac{c_E c_S(k_1 c_S + k_{-1})}{k_1(K_G + c_S)^2}e^{-k_1(K_G + c_S)t}$$

$$(37)$$

$$v_L(t) = \frac{V_L c_S}{(K_G + c_S)} + \frac{c_E c_S(k_1 c_S + k_{-1})}{(K_G + c_S)}e^{-k_1(K_G + c_S)t} \qquad (38)$$

By using a similar procedure for the other properties and equations, the remaining relationships were calculated as follows:

$$v_{-1}(t) = \frac{k_{-1} c_E c_S}{(K_G + c_S)} - \frac{k_{-1} c_E c_S}{(K_G + c_S)}e^{-k_1(K_G + c_S)t} \qquad (39)$$

$$x_{-1}(t) = \frac{k_{-1} c_E c_S}{k_1(K_G + c_S)^2} - \frac{k_{-1} c_E c_S}{(K_G + c_S)}t - \frac{k_{-1} c_E c_S}{k_1(K_G + c_S)^2}e^{-k_1(K_G + c_S)t} \quad (40)$$

and,

$$v_1(t) = \frac{(k_{-1} + k_2)c_E c_S}{(K_G + c_S)} + \frac{k_1 c_E c_S^2}{(K_G + c_S)} e^{-k_1(K_G + c_S)t} \tag{41}$$

$$x_1(t) = \frac{c_E c_S^2}{(K_G + c_S)^2} + \frac{(k_{-1} + k_2)c_E c_S}{(K_G + c_S)} t - \frac{c_E c_S^2}{(K_G + c_S)^2} e^{-k_1(K_G + c_S)t} \tag{42}$$

3 Results and discussion

3.1 Application and validation of the model

Figure 1a shows the non-linear adjustment of Eq. 36 (line) to product formation (tetraguaiacol) as described in the Methods. By recalling that x_2 represents the product, a non-linear adjustment was done with this equation, as shown below, where:

$$x_2(t) = \\ -\frac{k_1 k_2 c_E c_S}{(k_1 c_S - k_{-1} + k_2)^2} + \frac{k_1 k_2 c_E c_S}{(k_1 c_S - k_{-1} + k_2)} t + \frac{k_1 k_2 c_E c_S}{(k_1 c_S - k_{-1} + k_2)^2} e^{-(k_1 c_S - k_{-1} + k_2)t}$$

Considering that:

$$\phi_1 = k_1 k_2 c_E c_S \quad \text{and,} \tag{43}$$
$$\phi_2 = k_1 c_S - k_{-1} + k_2 \tag{44}$$

the previous equation becomes:

$$x_2(t) = -\frac{\phi_1}{\phi_2^2} + \frac{\phi_1}{\phi_2} t + \frac{\phi_1}{\phi_2^2} e^{-\phi_2 t} \tag{45}$$

Thus, to obtain the values for the fitting parameters ϕ_1 and ϕ_2 in Eq. (45), we ran a non-linear adjustment of the experimental data (Fig. 1a) using Eq. (45) for each substrate concentration to yield ϕ_1 and ϕ_2 for each condition. This figure also shows that the parameters ϕ_1 and ϕ_2 are dependent on the substrate concentration. Based on this finding, we introduced a second adjustment of the data, as shown in Fig. 1b (always done with MatLab software). In this case, we used Eqs. (43) and (44) to fit the data in Fig. 1b in order to express the dependence of the ϕ parameters on substrate concentration. However, since the reaction mixture consists of enzyme and other biological compounds, we concluded that the free substrate concentration in solution should be different from the total substrate concentration added to the solution. The total substrate added to the solution should be given by the following equation:

$$c_{TS} = c_{FS} + c_{LS} \tag{46}$$

where c_{TS} is the total substrate concentration added in the experiment, c_{FS} is the free substrate concentration and c_{LS} is the 'loosed' substrate concentration in the medium due to the action of others proteins in solution.

Recalling that the substrate concentration in all of the previous equations was assumed to be the *free substrate concentration*, it follows that:

$$\phi_1 = k_1 k_2 c_E c_{FS} = k_1 k_2 c_E c_{TS} - k_1 k_2 c_E c_{LS} \tag{47}$$

and from the parameter ϕ_2 the substrate dependency is given by

$$\phi_2 = k_1 c_{FS} - k_{-1} + k_2 = k_1 c_{TS} - k_1 c_{LS} - k_{-1} + k_2 \tag{48}$$

By performing a second linear fit of ϕ versus c_{TS} using Eqs. (47) and (48), the respective slopes (ψ_1, ψ_1') and intercepts (ψ_2, ψ_2') can be obtained for each parameter, as well as the residuals of these fittings (Fig. 2). Thus, for Eq. (47), we have:

$$\phi_1 = k_1 k_2 c_E c_{TS} - k_1 k_2 c_E c_{LS} = \psi_1 c_{TS} - \psi_2, \quad \text{so that} \tag{49}$$

$$\psi_1 = k_1 k_2 c_E \quad \text{and} \tag{50}$$

$$\psi_2 = k_1 k_2 c_E c_{LS} \tag{51}$$

Similarly, for Eq. (48), we obtain:

$$\phi_2 = k_1 c_{TS} - k_1 c_{LS} + k_{-1} + k_2 = \psi_1' c_{TS} - \psi_2', \quad \text{so that} \tag{52}$$

$$\psi_1' = k_1 \text{ and} \tag{53}$$

$$\psi_2' = k_1 c_{LS} + k_{-1} - k_2 \tag{54}$$

After the linear adjustment of Eqs. (49) and (52), we finally obtain the ψ properties of parameters ϕ_1 and ϕ_2 that allow calculation of the kinetic properties of the system. From the slope and intercept of Fig. 2a, b using ϕ_1 and ϕ_2 (Eqs. 49 and 52, respectively), the ψ properties can be obtained. The results obtained are given in the respective legends, which also describe the conditions necessary to determine all of the parameters of the Michaelis–Menten model. For pineapple POD, this analysis yielded:

$$k_1 = \psi'_1 = 1.0993\, s^{-1} \tag{55}$$

$$\psi_1 = k_1 k_2 c_E \Rightarrow k_2 = \frac{\psi_1}{k_1 c_E} = 2.6166\, s^{-1} \tag{56}$$

$$\psi_2 = k_1 k_2 c_E c_{LS} \Rightarrow c_{LS} = \frac{\psi_2}{k_1 k_2 c_E} = 7.9537 \times 10^{-3} (\text{mol/L}), \text{ and} \tag{57}$$
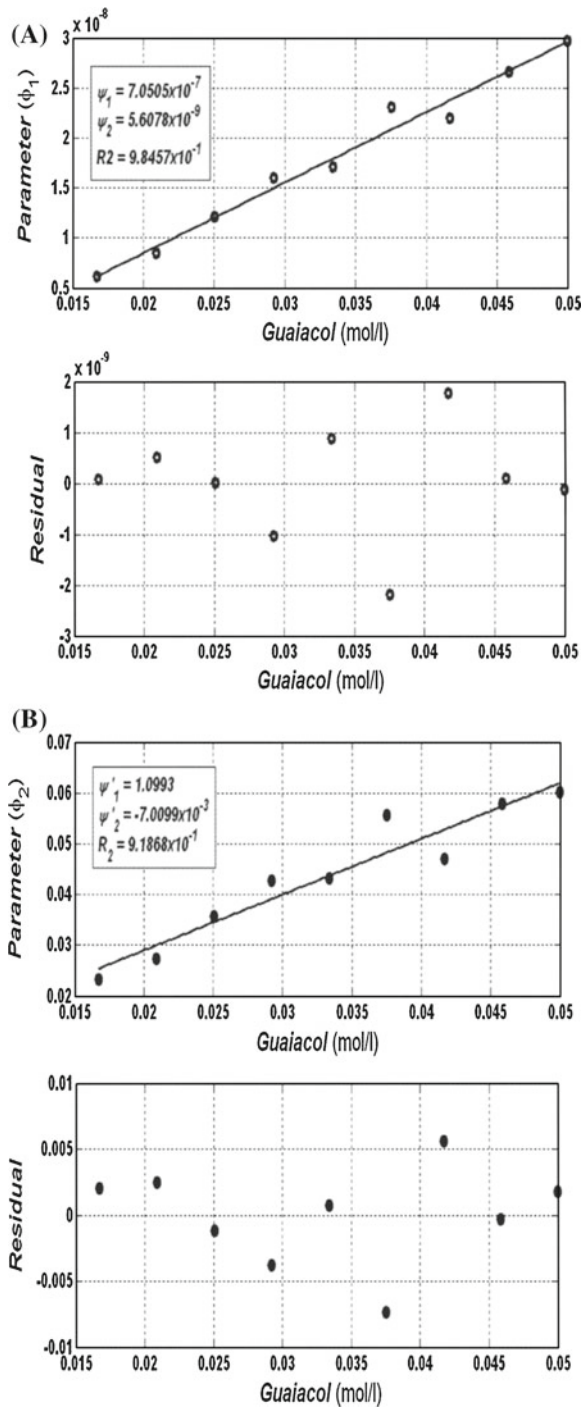
$$k_{-1} = k_2 - k_1 c_{LS} + \psi'_2 = 2.6009\, s^{-1} \tag{58}$$

$$K_G \equiv K_M = 1.4330 \times 10^{-2} \tag{59}$$

$$V_M = 6.4134 \times 10^{-7} (\text{mol/s}) \tag{60}$$

Equations (55–60) allow calculation of all of the properties of the Michaelis–Menten model and the Monod model for fermentation. Hence, for the first time it is possible

to obtain all the rate constants of this model as well as the amount (in this case) of loosed substrate. In this view, when the amount of loosed substrate is close to zero, i.e., $c_{FS} \cong c_{TS}$, the medium in which this occurs does not cause significant loosening of the total substrate concentration added due to the absence of others compounds that bind the substrate. In addition, the results obtained here allow the calculation of any three dimensional surface from the average point of view since the second fitting furnishes the mean behavior of the parameters ϕ_1 and ϕ_2. Thus, all the velocities, extent of reactions and, consequently, the species concentration are dependent only on the previous parameters. Analysis of the results obtained here clearly shows how this approach can be used to optimize catalytic processes, including fermentation. For instance, analysis of Figs. 1a and 3a shows that while Fig. 1a furnishes the individual behavior of product formation that best fits the experimental data, Fig. 3a provides results based on all of the data collected.

To demonstrate how optimization can be reached by this new approach, consider two situations presented in the level diagrams. In the first situation (based on the data in Fig. 3b), when the total substrate concentration is 0.03 mol/L and the reaction time
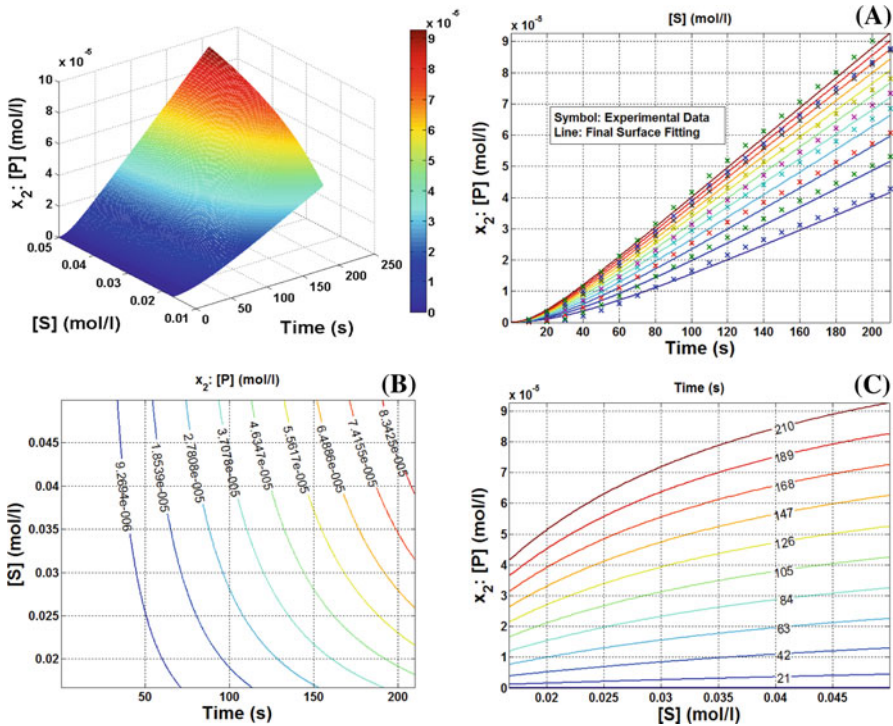

Fig. 3 Surface adjustment of the overall experimental data for product (*P*) versus time at different substrate concentrations. **a** Individual adjustment obtained from fitting Eqs. (45) and (49) to the theoretical and experimental data obtained for the plot of product versus time at different substrate concentrations. **b** Level diagrams obtained from cuts of the surface data for the plot of substrate versus time at different product concentrations. **c** Level diagrams obtained from the surface data for the plot of product versus substrate concentration at different reaction times
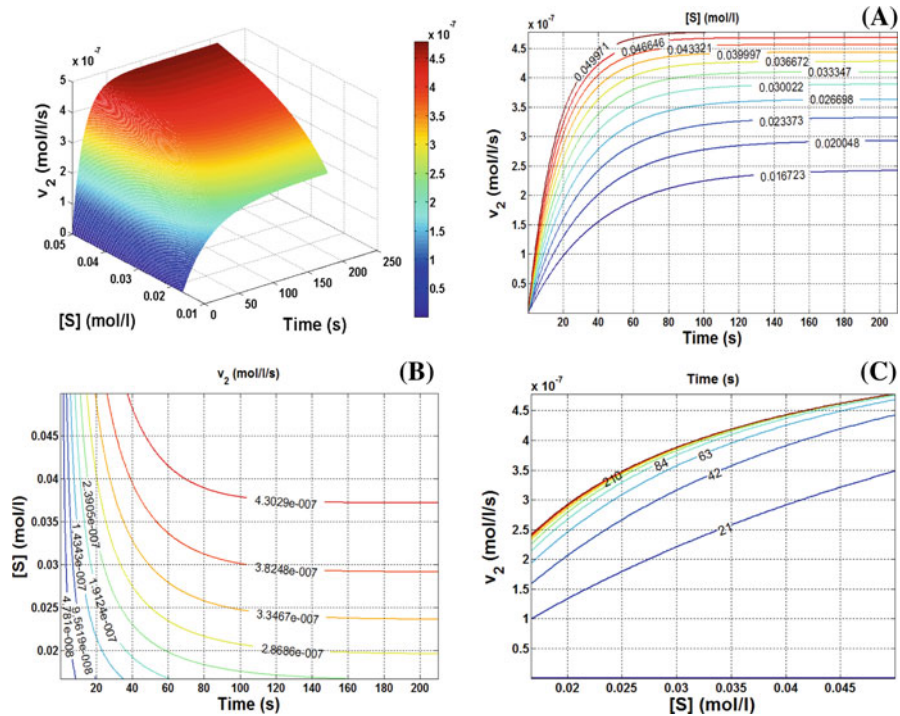
Fig. 4 Surface response of the overall data for the velocity of product formation (v_2) versus time and substrate concentration. **a** Level diagrams obtained from the theoretical plot of cuts of the surface data for velocity of product formation versus time at different substrate concentration. **b** Level diagrams obtained from cuts of the surface data for the plot of substrate versus time at different velocities of product formation. **c** Level diagrams obtained from cuts of the surface data for the plot of the velocity of product formation versus substrate concentration at different reaction times

is 120 s, the total product formation obtained is 3.70×10^{-5} mol/L (Fig. 3b). Using the same substrate concentrations and times in Fig. 4a shows that for these conditions the velocity of product formation (v_2) is ∼3.85×10^{-7} mol/L/s. Similarly, Fig. 5a shows that the total amount of complex (ES) is ∼1.47×10^{-7} mol/L and from Fig. 6a the amount of free enzyme observed (E) is ∼9.78×10^{-8} mol/L. These results lead to the conclusion that the total amount of enzyme needed in solution is the sum of ES and E, i.e., 2.45×10^{-7} mol/L. For fermentation processes, the total biomass needed in solution is obtained by the same procedure as described above. Figure 6 shows the remainder of the reaction and the corresponding velocities which, in this case, were $x_1 = 7.54 \times 10^{-5}$ mol/L, $v_1 = 7.74 \times 10^{-7}$ mol/L/s, $x_{-1} = 3.82 \times 10^{-5}$ mol/L, $v_{-1} = 3.88 \times 10^{-7}$ mol/L/s, $x_L = 3.72 \times 10^{-5}$ mol/L and $v_L = 3.85 \times 10^{-7}$ mol/L/s.

This first analysis provided data from which it was possible to obtain the desired amount of product (3.7×10^{-5} mol/L) (Fig. 3b). However, inspection of Fig. 3b shows that this is not the only way to reach this concentration. When one is interested in producing this amount of product using the cheapest process it is necessary to know what makes this process more expensive.

In the second situation, in which the substrate concentration makes product formation more expensive, optimization of the process will lead to conditions in which a low substrate concentration is used. Figure 3b shows that the same amount of product formation can be obtained using a total substrate concentration of 0.02 mol/L and reaction time of 160.5 s. This will require only 67% of the substrate concentration used in the first case. Using these new values for substrate concentration and time in Fig. 4a, the velocity of product formation (v_2) is $2.90 \times, 10^{-7}$ (mol/L/s). Similarly, Fig. 5a shows that the total amount of ES formed is 1.11×10^{-7} mol/L, and from Fig. 5d the amount of E is 1.34×10^{-7} mol/L. As before, these results lead to the conclusion that the total amount of enzyme needed in solution is the sum of the amount of ES and E, which is 2.45×10^{-7} mol/L. Comparison of the total amount of enzyme calculated here with the first case shows that the amount required is the same in both
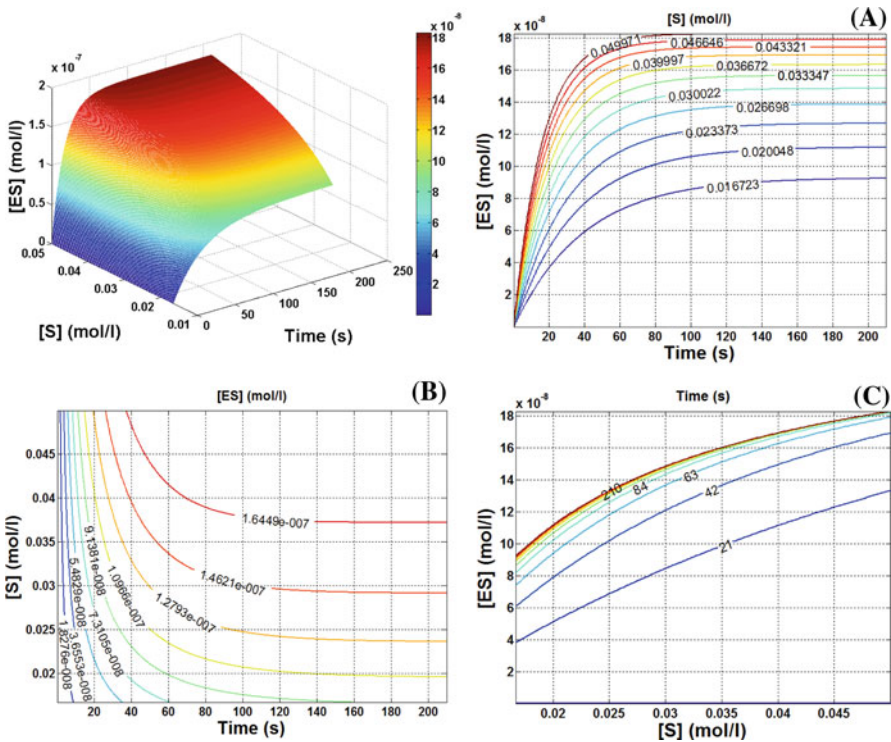

Fig. 5 Surface response of the overall data for complex (ES) formation versus time and substrate concentration. **a** Level diagrams obtained for the theoretical plot obtained from cuts of the surface data for ES formation versus time at different substrate concentrations. **b** Level diagrams obtained from cuts of the surface data for the plot of substrate versus time at different amounts of ES formation. **c** Level diagrams obtained from the surface data for the plot of ES formation versus substrate concentration at different reaction times. Next, surface response of the overall data for the free enzyme (E) concentration versus time and substrate concentration. **d** Level diagrams obtained for the theoretical plot obtained from the surface data for the concentration of E versus time at different substrate concentrations. **e** Level diagrams obtained from the surface data for the plot of substrate versus time at different concentrations of E. **f** Level diagrams obtained from the surface data for the plot of the concentration of E versus substrate concentration at different reaction times
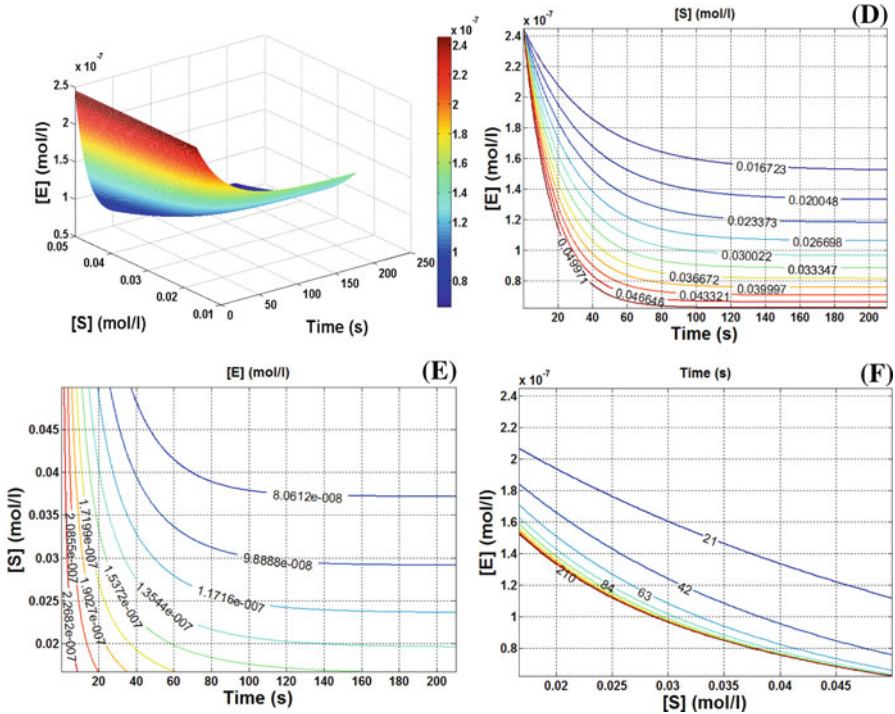
Fig. 5 continued

cases and, consequently, the amount of enzyme needed will not make this process more expensive. Thus, as in the first case, the total biomass needed in solution should be obtained in the same was as in fermentation processes. Figure 6 can be used to determine the extent of reaction and its velocities for this second situation, i.e., $x_1 = 8.15 \times 10^{-5}$ mol/L, $v_1 = 6.24 \times 10^{-7}$ mol/L/s, $x_{-1} = 4.44 \times 10^{-5}$ mol/L, $v_{-1} = 3.34 \times 10^{-7}$ mol/L/s, $x_L = 3.71 \times 10^{-5}$ mol/L and $v_L = 2.90 \times 10^{-7}$ mol/L/s.

Based on the results for these two cases, we conclude that the velocity of product formation in the second case was lower than in the first case whereas the enzyme concentration was identical in both cases. However, a longer reaction time is now required and must be considered during the optimization process. The reduction in the cost of product formation will be related to the length of the reaction time and especially to the substrate concentration used. Such an evaluation can also be made using the level diagrams presented in the respective figures or directly from the MatLab program.

Another important point in using this approach relates to the number of data points used in Lineweaver–Burk plots (1/v vs. 1/s) (not shown). The usual procedure in most analyses is to discard the initial points that are nonlinear. When some initial points are discarded, i.e., an increase in the number of discarded points makes the plot linear only at high substrate concentrations. This kind of plot is accurate only for a short interval of 1/s. This means that the common procedure of eliminating certain points leads to deviation of the experimental results since the steady-state point that is chosen will
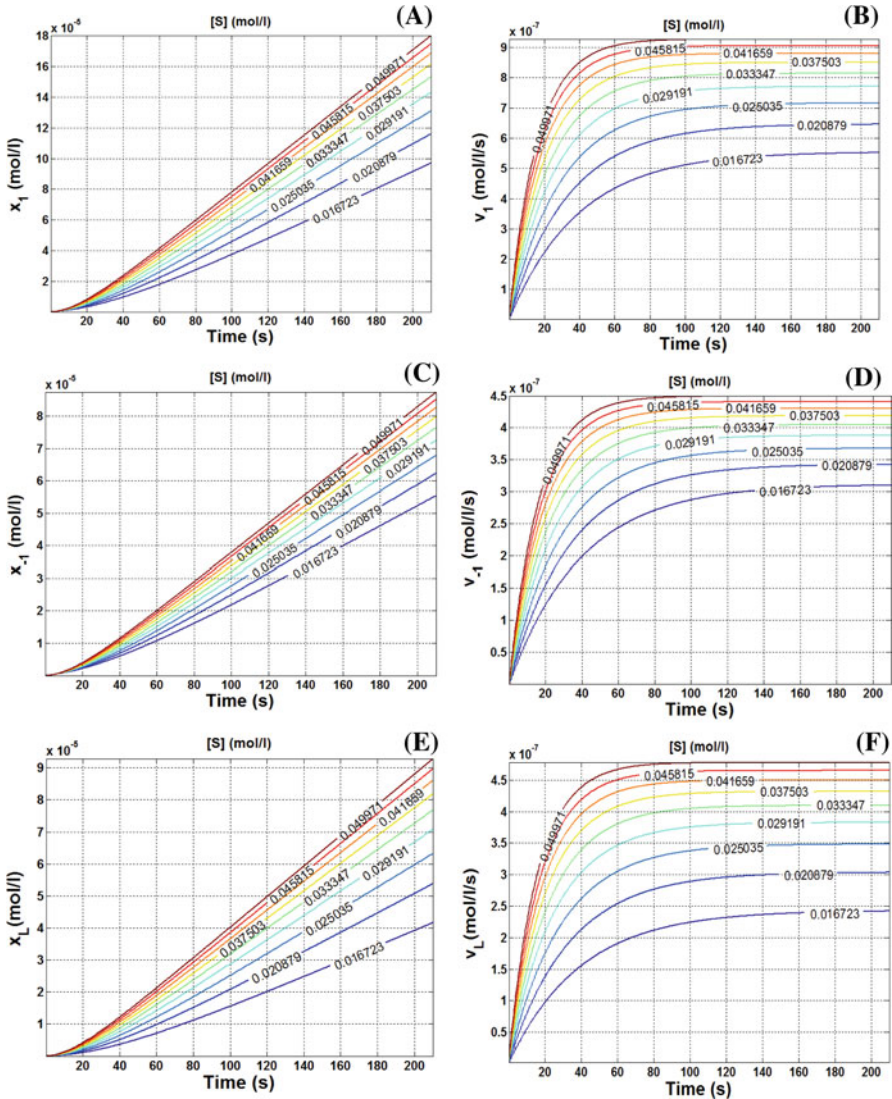
Fig. 6 **a** Theoretical results obtained for the extent of reaction (x_1) based on the theoretical data of pineapple peroxidase at different substrate concentrations. The remaining panels show the theoretical results obtained for **b** the velocity of reaction (v_1), **c** the extent of reaction (x_{-1}), **d** the velocity of reaction (v_{-1}), (**e**) the net extent of reaction (x_L) and (**f**) the net velocity of reaction (v_L) at different substrate concentrations

change with time for each substrate concentration. In contrast, the present treatment is more accurate since all of the points are considered by the fitted equation at any time point.

   To date there has been no report of an analytical solution that describes the initial Briggs–Haldane approach without assuming the steady-state condition. The possibility of solving this model without the steady-state constraint but based on the extent of reaction (x) provides a powerful new tool for understanding the function, energy and

dynamics of biomolecules and microorganisms. The relationship that describes micro-organism growth resembles the Michaelis–Mentem approach but was formalized by Monod [21]. The shape of the Monod curve is identical to that for Michaelis–Menten enzyme kinetics, which makes sense because in most cases the kinetics of growth is limited by the activity of a permease responsible for transporting substrate into the cell [22]. Thus, in processes involving microorganisms, it should be possible to apply equations derived from the equation proposed by Monod [23,24], thus expanding our recent concepts. Although solving this model by Laplace transforms may seem complex, application of the resulting equations is very simple. This is so because to apply the equations of this method requires nonlinear fitting that involves only two unknown parameters (ϕ_1 and ϕ_2) in the first adjustment, and, two linear fittings of the ϕ parameters in the second adjustment. With regard to improvements in kinetic theory, the traditional approach based on steady-state kinetics yields only values for K_M and V_M based on plots like that of Lineweaver and Burk [25]. In contrast, the procedure described here generates these two parameters and several others, such as values for k_1, k_{-1} and k_2, thereby allowing complete characterization of this model when the substrate concentration is much higher than the enzyme concentration.

4 Conclusion

The most important finding of this work is the description of an analytical solution for the classic Michaelis–Menten and Monod models, with the first of these having been analyzed by Briggs and Haldane, without their restriction of a steady-state condition. A classic example of the need for the kind of information provided by the present treatment is the production of bacteria and yeast for veterinary vaccines and product formation. From an industrial point of view, the use of this procedure will furnish crucial information on the influence of pH, ions, temperature, enzyme concentration and other assay parameters that can be used to improve yields in enzyme-based processes.

References

1. C. O'Sulivan, S.W. Tompson, J. Chem. Soc. Faraday Trans. **57**, 834 (1890)
2. A. Cornish-Bowden, *Fundamentals of Enzyme Kinetics* (Portland Press, London, 2004)
3. G.C. Brown, J. Chem. Soc. Faraday Trans. **61**, 369 (1892)
4. V. Henri, CR. Hebd. Seanc. Acad. Sci. **135**, 916 (1902)
5. V. Henri, *Lois Générale de l'Action de Diastase* (Hermann, Paris, 1903)
6. L. Michaelis, M.L. Menten, Biochem. Zeit. **49**, 333 (1913)
7. G. Briggs, J. Haldane, Biochem. J. **19**, 338 (1925)
8. Q.H. Gibson, Method. Enzymol. **16**, 187 (1969)
9. C. Ajila, U. Rao, J. Mol. Catal. B Enzym. **60**, 36 (2009)
10. J.C. Leon, I.S. Alpeeva, T.A. Chubar, I.Y. Galaev, E. Csoregi, I.Y. Sakharov, Plant Sci. **163**, 1011 (2002)

11. A.S.L. Carvalho, E.P.E. Melo, B.S. Ferreira, M.T. Neves-Petersen, S.B. Petersen, M.R. Aires-Barros, Arch. Biochem. Biophys. **415**, 257 (2003)
12. L. Wang, K. Burhenne, B. Kristensen, S. Rasmussen, Gene **343**, 323 (2004)
13. S. Johri, U. Jamwal, S. Rasool, A. Kumar, V. Verma, G.N. Qazi, Plant Sci. **169**, 1014 (2005)
14. A. Rosenthal, D. Ledward, A. Defaye, S. Gilmour, L. Trinca, Trends HP Biosci. Biotech. **19**, 525 (2002)
15. E. Agostini, J. Hernandez-Ruiz, M.B. Arnão, S.R. Milrand, H.A. Tigier, M. Acosta, Biotechnol. Appl. Biochem. **35**, 1 (2002)
16. E. Morales-Blancas, V. Chandia, L. Cisneros-Zevallos, J. Food Sci. **67**, 146 (2002)
17. E. Antonini, M. Brunori, *Hemoglobin and Myoblobin in their Reactions with Ligands* (North Holland Publishing Company, London, 1971)
18. S. Aibara, H. Yamashita, E. Mori, M. Kato, Y. Morita, J. Biochem. **92**, 531 (1982)
19. E. Kreyszig, *Matemática Superior para Engenharia* (LTC, Rio de Janeiro, 2009)
20. W. Schmidell, U.A. Lima, E. Aquarone, W. Borzani, *Industrial Biotechnology* (Ed. Edgar Blücher, São Paulo, 2001)
21. J. Monod, The growth of bacterial cultures. Annu. Rev. Microbiol. **3**, 371 (1949)
22. M. Fonseca, J.A. Teixeira, *Reactores Biológicos* (Lidel, Lisboa, Porto, 2007)
23. D. Silva, T. Branyik, G. Dragone, A.A. Vicente, J.A. Teixeira, J.B Almeidae Silva, Chem. Pap. **62**, 34 (2008)
24. G.B.M. Carvalho, D.P. Silva, C.V. Bento, A.A. Vicente, J.A. Teixeira, M.G. Felipe, J.B. Almeidae Silva, Appl. Biochem. Biotechnol. **155**, 55 (2009)
25. H. Lineweaver, D. Burk, J. Am. Chem. Soc. **56**, 658 (1934)